HHS Public Access

Author manuscript

Mult Scler. Author manuscript; available in PMC 2021 October 01.

Published in final edited form as:

Mult Scler. 2020 October ; 26(12): 1497–1509. doi:10.1177/1352458519867320.

Profiles of cortical inflammation in multiple sclerosis by ^{11}C-PBR28 MR-PET and 7 Tesla imaging

Elena Herranz, PhD[1,2], **Celine Louapre, MD, PhD**[1,2], **Constantina Andrada Treaba, MD, PhD**[1,2], **Sindhuja T Govindarajan, MS**[1], **Russell Ouellette**[1], **Gabriel Mangeat, MS**[1,3], **Marco L Loggia, PhD**[1,2], **Julien Cohen-Adad, PhD**[3], **Eric C. Klawiter, MD**[2,4], **Jacob A. Sloane, MD, PhD**[2,5], **Caterina Mainero, MD, PhD**[1,2]

[1]Athinoula A. Martinos Center for Biomedical Imaging, Massachusetts General Hospital, Department of Radiology, Boston, MA, USA

[2]Harvard Medical School, Boston, MA, USA

[3]Institute of Biomedical Engineering, Polytechnique Montreal, Montreal, QC, Canada

[4]Department of Neurology, Massachusetts General Hospital, Boston, MA, USA

[5]Department of Neurology, Beth Israel Deaconess Medical Center, Boston, MA, USA

Abstract

Background.—Neuroinflammation with microglia activation is thought to be closely related to cortical MS lesion pathogenesis.

Objective.—Using ^{11}C-PBR28 and 7 Tesla (7T) imaging, we assessed in 9 RRMS and 10 SPMS patients 1) microglia activation in lesioned and normal appearing cortex, 2) cortical lesion inflammatory profiles; 3) the relationship between neuroinflammation and cortical integrity.

Methods.—Mean ^{11}C-PBR28 uptake was measured in focal cortical lesions, cortical areas with 7T quantitative T_2* (q-T_2*) abnormalities, and normal appearing cortex. The relative difference in cortical ^{11}C-PBR28 uptake between patients and 14 controls was used to classify cortical lesions as either active or inactive. Disease burden was investigated according to cortical lesion inflammatory profiles. The relation between q-T_2* and ^{11}C-PBR28 uptake along the cortex was assessed.

Results.—^{11}C-PBR28 uptake was abnormally high in cortical lesions in RRMS and SPMS; in SPMS, tracer uptake was significantly increased also in normal appearing cortex. ^{11}C-PBR28 uptake and q-T_2* correlated positively in many cortical areas, negatively in some regions. Patients with high cortical lesion inflammation had worse clinical outcome and higher intracortical lesion burden than patients with low inflammation.

Conclusions.—^{11}C-PBR28 and 7T imaging reveal distinct profiles of cortical inflammation in MS, which are related to disease burden.

Corresponding author: Caterina Mainero, MD, PhD, Athinoula A. Martinos Center for Biomedical Imaging, 149, Thirteenth Street, Charlestown, MA 02129, caterina@nmr.mgh.harvard.edu, Phone: (+1) 617-724-7746, Fax: (+1) 617 726-7422.

Conflicts of Interest

The authors declare no conflicts of interest.

Keywords

multiple sclerosis; microglia; inflammation; positron emission tomography; ^{11}C-PBR28; cortical lesions; demyelination; 7 Tesla MRI; T_2* relaxometry

Introduction

Cortical demyelination is a major determinant of multiple sclerosis (MS) progression[1, 2].

Meningeal inflammation with microglia activation is thought to represent a main driver of cortical MS demyelination[3, 4]. Activated microglia upregulate expression of the 18kDa translocator protein (TSPO), which can be imaged by selective positron emission tomography (PET) radioligands[5]. Initial PET studies demonstrate cortical TSPO upregulation in relapsing-remitting and secondary-progressive MS (RRMS, SPMS) cases[6, 7], which overall correlates with worse clinical outcome. It is still unclear whether microglia activation is a homogenous process across the cortex or whether different inflammation levels can be detected within cortical lesions and individual patients.

In white matter (WM), “smoldering” plaques with active microglia at the lesion periphery show progression of tissue damage[8-10]. While the criteria for histological characterization of WM lesion activity are well established[11] there is no consensus for staging cortical lesion activity.

We combined ^{11}C-PBR28, a second-generation TSPO PET radiotracer, with 7 Tesla (7T) MRI, which shows increased sensitivity to focal and diffuse microstructural cortical pathology[12,13], to characterize neuroinflammation in lesioned and normal appearing cortex of RRMS and SPMS patients. Lesioned cortical tissue was defined as either focal lesions or quantitative T_2* (q-T_2*) abnormalities at 7T. We hypothesized that: i) in earlier MS neuroinflammation co-localizes with cortical lesions; in later stages it extends to normal appearing cortex; ii) TSPO quantification can be used to stage cortical lesion inflammatory activity *in vivo* and identify distinct patient profiles of cortical inflammation, with different disease burden.

Finally, we investigated in patients the relationship between cortical microstructural integrity and microglia activation.

Materials and methods

Standard Protocol Approvals, Registrations, and Patient Consents

The Institutional Review Board and the Radioactive Drug Research Committee approved study procedures; written informed consent was obtained for all subjects. To maintain subjects’ confidentiality, we assigned each subject a study code, kept all records in locked security cabinets. Only subjects’ information important for the study conduct was distributed to study staff; data were stored in a password-protected computer, available only to investigators.

Subjects—Twenty-three MS patients were prospectively recruited from a cohort of 27 MS cases who were genotyped for the Ala147Thr polymorphism in the TSPO gene, which predicts binding affinity to ^{11}C-PBR28[14]. Only subjects with Ala/Ala (high-affinity binders, HAB) and Ala/Thr (mixed-affinity binders, MAB) genotypes underwent subsequent ^{11}C-PBR28 MR-PET and 7T imaging. Four patients were subsequently excluded due to the presence of motion artifacts at 7T. The final cohort included 10 SPMS and 9 RRMS patients.

We enrolled 17 age-matched healthy controls for comparisons with 7T data, and additional 14 age-matched healthy controls for comparison with PET data. Inclusion criteria for MS: age between 18-65 years; diagnosis of clinically definite MS; education ≥ 8 years; absence of clinical relapse within 3 months, corticosteroids therapy within one month from enrollment. General exclusion criteria: benzodiazepines treatment, PET/MRI contraindications, major medical disorders (other than MS for patients).

In patients, within 1 week from imaging procedures, neurological disability was assessed using the Expanded Disability Status Scale (EDSS), and cognitive performance with Symbol Digit Modalities (SDMT). SDMT raw scores were converted to Z-scores after correcting for age and education[15].

Imaging data acquisition

MR-PET—Patients and 14 controls matched for TSPO affinity underwent 90-minute ^{11}C-PBR28 MR-PET imaging on a Siemens integrated 3T MR-PET system (BrainPET), with a spatial resolution of ~2.8 mm in the center of the field of view[16]. PET data were acquired after receiving an intravenous bolus injection of ^{11}C-PBR28 produced in-house (mean±SD administrated dose 11.5±0.7mCi in MS versus 11.7±0.5mCi in controls, p= 0.1 by unpaired t-test), as previously described[7]. A structural 3D-magnetization-prepared rapid scan with multiple gradient-echoes (MEMPR) images (voxel size=1mm isotropic)[17] was acquired simultaneously to PET data for cortical surface reconstruction, generation of attenuation correction maps[18], coregistration to PET and 7T data, and cortical thickness estimation.

7T MRI—The 7T MRI protocol obtained in patients and 17 controls included: 1) multi-echo 2D-dimensional T_2*-weighted spoiled gradient-echo images (TR=2210ms, TE=6.44+3.32n [n=0,...,11]ms, resolution=0.33×0.33×1mm^3, 25% gap) for assessing q-T_2* at different cortical depths; 2) T_1-weighted 3D magnetization-prepared rapid acquisition gradient-echo sequence (TR/TI/TE=2600/1100/3.26ms, resolution=0.60×0.60×1.5mm^3) for co-registration of 7T gradient-echo data with cortical surfaces; 3) single-echo T_2*-weighted spoiled gradient-echo pulse sequence (resolution=0.33×0.33×1mm^3, 25% gap) for cortical lesion segmentation[13].

Imaging data processing

An overview of the imaging processing is summarized in Figure 1.

Cortical surface reconstruction—Pial and WM surface reconstruction and cortical thickness estimation were performed in the 3D MEMPR volume[18] using FreeSurfer, v5.3,

which includes an in-house semi-automated lesion filling method to correct topological defects in cortical surface reconstruction due to WM and/or leukocortical lesions.

Quantitative T_2* at 7T—Quantitative T_2* maps were generated from 7T multi-echo T_2* scans as previously described[9], registered onto the corresponding 3T cortical surfaces with boundary-based registration, concatenated into a whole brain volume using FreeSurfer tools (voxel size=0.3mm^3 isotropic)[19]. Due to the diffuse cortical pathology reported at different cortical depths by previous 7T in vivo data[20], q-T_2* maps were sampled at 25%, 50% and 75% depth from the pial surface (0%) to the GM/WM boundary (100%).

Lesion segmentation—Cortical and WM lesions were segmented by consensus of two experienced raters using Slicer, v4.2.0. Focal cortical lesions were defined as cortical hyperintensities extending for at least 3 voxels across two consecutive slices on 7T single-echo T_2* acquisitions (Figure 2), and classified as either intra- or leuko-cortical, as previously detailed[13]. Intracortical and leukocortical lesion types were grouped since previous investigations did not find differences in intracortical TSPO expression[7]. Cortical lesion distribution maps in patients were obtained using FreeSurfer, as previously detailed[13].

Quantification of ^{11}C-PBR28 binding—Cortical ^{11}C-PBR28 binding was assessed using standardized uptake values (SUV). In-house software was used to compute voxel-wise, for each subject, SUV (mean radioactivity/injected dose/weight) from the 60-90 minutes post-injection data, as previously described[7]. PET data were reconstructed using 3D-ordinary Poisson ordered-subset expectation maximization reconstruction, with corrections for attenuation, scattering, random coincidences, dead-time, sensitivity and normalization.

To account for global signal differences across subjects, SUV maps were normalized by a pseudoreference region (SUVR) in normal appearing WM with mean SUV in patients around the mean SUV in controls, as previously reported[7]. We demonstrated that SUVR estimated with this method strongly correlate with the volume of distribution of the same tracer[7]. Since MS patients and controls show similar levels of ^{11}C-PBR28 plasma concentrations, and no differences in the area under the blood curves[21], the use of SUVR is a reliable approach to assess brain tracer uptake.

To minimize partial volume effects, cortical SUVR were sampled at the surface-based level, at mid-cortical depth, as previously detailed[7].

Statistics

Statistical analyis was performed with R software (v2.13.1). Demographics were compared between patients and controls using Mann-Whitney U-test or χ^2 test.

A general linear model (GLM) was used in FreeSurfer to assess differences in cortical q-T_2* at 25%, 50%, 75% depth from the pial surface in either RRMS or SPMS relative to controls. In cortical areas showing q-T_2* differences, the corresponding ^{11}C-PBR28 SUVR were also extracted.

To identify active and inactive cortical lesions based on ^{11}C-PBR28 uptake, the presence of significant differences in cortical ^{11}C-PBR28 SUVR between patients and controls was assessed using GLM surface-based analysis by sampling SUVR at 50% depth from the pial surface. From this analysis, several cortical regions of increased SUVR were identified in MS versus controls. From these areas, the relative difference in the mean cortical ^{11}C-PBR28 SUVR between patients and controls was estimated, separately for MAB and HAB, and used as threshold to classify each cortical lesion as active, if its mean SUVR extracted at mid-cortical depth was greater than the calculated threshold, or inactive with mean SUVR below the threshold. A similar approach has been previously used to measure TSPO expression in WM MS lesions[22]. The median volume of active cortical lesions was calculated in the whole MS cohort, and used to group patients into two categories: 1) high inflammatory cortical lesion activity, if the total volume of active cortical lesions in that individual MS patient was≥ the median and 2) low inflammatory cortical lesion activity, if lower than the median. Differences in demographic, clinical and structural MRI metrics between patients with high and low inflammatory cortical lesion activity were investigated using Mann-Whitney U-test.

In each MS group (RRMS, SPMS) mean SUVR in cortical regions with abnormally increased q-T_2*, as well as in active and inactive cortical lesions were compared to i) mean SUVR in normal appearing cortex within patients using paired t-test, ii) mean cortical SUVR in controls using multivariate linear regression. Multilinear regression analysis was also used to compare iii) in both patient groups mean SUVR in normal appearing cortex with mean cortical SUVR in healthy controls, and iv) mean SUVR in all cortical regions between RRMS and SPMS.

Finally, a vertex-wise GLM was run in FreeSurfer to assess across the whole cortex in patients the relationship between ^{11}C-PBR28 uptake and q-T_2* sampled at 50% cortical depth from the pial surface.

Age and ^{11}C-PBR28 affinity binding were included as adjustment variables in both multilinear regression and GLM analyses. Prior to all surface-based analyses, q-T_2* and ^{11}C-PBR28 surfaces were normalized to “fsaverage” in Freesurfer and smoothed using a 5 mm and 10 mm full width at half maximum Gaussian kernel, respectively. A clusterwise correction for multiple comparisons was applied in GLM analyses using Monte-Carlo simulation with 10,000 iterations.

Results

Demographics and clinical data

Study demographic and clinical data are shown in Table 1. Fourteen out of 19 patients were on stable (at least 6 months) treatment with disease modifying agents.

Cortical lesions and q-T_2* changes at 7T

Structural MRI metrics for the cortex and WM are reported in Table 1. Cortical lesions were identified in 7 RRMS and 10 SPMS patients. Cortical lesion distribution maps are illustrated in Figure 3A.

The GLM laminar analysis disclosed in both RRMS and SPMS areas of abnormally increased q-T_2* ($p < 0.05$), indicative of myelin and/or iron loss, which were diffuse across the cortex (Figure 3B). We did not find any cortical region with decreased q-T_2* in either RRMS or SPMS compared to controls.

^{11}C-PBR28 uptake in lesioned and normal appearing cortex

In RRMS, 42% of the total cortical lesions were active. Mean ^{11}C-PBR28 SUVR in active cortical lesions and in regions with abnormally increased q-T_2* were higher than mean ^{11}C-PBR28 SUVR in normal appearing cortex and mean cortical ^{11}C-PBR28 SUVR in controls (Figure 4A, Table 2). Mean ^{11}C-PBR28 SUVR in normal appearing cortex in RRMS did not differ from mean healthy control SUVR.

In SPMS, 62% of total cortical lesions were active. Mean ^{11}C-PBR28 SUVR in active cortical lesions and in areas with abnormally increased q-T_2* were higher than mean ^{11}C-PBR28 SUVR in normal appearing cortex and mean cortical ^{11}C-PBR28 SUVR in controls (Figure 4B, Table 2). Mean ^{11}C-PBR28 SUVR in normal appearing cortex were also higher than mean cortical ^{11}C-PBR28 SUVR in controls.

There were no differences in ^{11}C-PBR28 SUVR between RRMS and SPMS in any of the regions examined (Figure 4C).

Clinical and MRI burden characteristics in different inflammatory profiles of cortical lesions

There were no differences in age, disease duration, and binding affinity between patients with high versus low cortical lesion inflammation (Table 2). Patients with high cortical lesion inflammation showed, however, lower SDMT scores ($p = 0.02$) and increased EDSS ($p = 0.047$), as well as higher intracortical lesion burden ($p = 0.02$). No differences were found in cortical thickness and either leukocortical or WM lesion metrics. All patient groups disclosed cortical thinning relative to controls ($p < 0.05$ by multivariate linear regression adjusting for age).

Relationship between ^{11}C-PBR28 SUVR and laminar quantitative T_2* in the cortex

The GLM laminar analysis investigating the relationship between 7T q-T_2* and ^{11}C-PBR28 SUVR in RRMS and SPMS patients disclosed several areas of positive correlation ($p<0.05$) between ^{11}C-PBR28 uptake and q-T_2* (Figure 5). Areas of inverse correlation were also detected. In RRMS, the total surface area of regions of positive correlation, that is the higher ^{11}C-PBR28 SUVR the higher q-T_2*, was ~10 times greater than the area occupied by regions with negative correlation. In SPMS, however, the total surface of regions of negative correlation was twice greater than the total area with a positive correlation between ^{11}C-PBR28 SUVR and q-T_2* (Table 3).

To investigate whether q-T_2* was pathological in areas with either a negative or a positive association with SUVR, q-T_2* values were extracted from these regions, in each patient, and compared to the corresponding q-T_2* values in controls. In regions with either positive or

negative association between q-T_2* and SUVR, q-T_2* was abnormally higher than in healthy controls, indicating myelin and/or iron loss (Table 4).

Discussion

We combined MR-PET imaging with ^{11}C-PBR28, a marker of activated microglia, with 7T MRI to investigate the distribution and relevance of neuroinflammation in lesioned and normal appearing cortex in a heterogeneous MS cohort. “C-PBR28 PET has been used to reliably distinguish glial activation in neurological disorders from healthy individuals[7, 23, 24]. We found that in RRMS TSPO upregulation tends to co-localize with cortical lesion pathology; in SPMS, it extends beyond cortical lesions, suggesting progression of neuroinflammation. Our data also suggest that quantification of intracortical levels of TSPO expression could allow staging cortical lesion inflammatory activity *in vivo*. Patients with high inflammatory profiles exhibited lower cognitive performance, increased EDSS and higher intracortical lesion burden compared to patients with low inflammation. Interestingly, the two patient groups showed no differences in age, disease duration, and burden of WM and leukocortical lesions, suggesting that disease duration is not the primary correlate of disease burden and that the effects of neuroinflammation are dissociated in the cortex and WM, with the most detrimental effects occurring intracortically. No differences were observed in cortical thickness either, likely because it could result from both intracortical degeneration and disconnection from underlying WM lesions.

Neuropathological data demonstrate that microglia accumulate in a cytotoxic phenotype at sites of active demyelination in WM, and significantly drop in numbers and change to a homeostatic phenotype in inactive lesions[25]. Although similar processes have been suggested for cortical lesions[26], there is no established consensus for staging cortical lesion inflammatory activity. A specific CSF proinflammatory profile has been shown to be associated with high cortical lesion load on 3T MRI, suggesting that CSF analysis could help to identify patients at high risk of severe GM damage[4]. Our findings indicate that combined “C-PBR28 TSPO and 7T imaging could represent an alternative radiological tool for this purpose.

We investigated the presence of neuroinflammation in normal appearing cortex throughout MS stages. Previous ^{11}C-PK11195 PET data have reported abnormally increased cortical TSPO expression in MS patients[6]. We demonstrated that the combined used of ^{11}C-PBR28 MR-PET with 7T T_2* acquisitions allows measuring microglia activation in focal cortical lesions in MS[7]. The presence and role of microglia in normal appearing cortex have not been determined in these studies. Ultra-high field MRI doubles cortical lesion detection compared to lower field MRI[12]. Voxel-wise analyses of cortical myelin integrity significantly improve cortical lesions identification[12]. Among different approaches, surface-based analysis of q-T_2* at 7T as a function of cortical depth is reproducible[28] and can be used to disclose cortical abnormalities, likely related to changes in myelin and iron content, which extend beyond visible cortical MS lesions[13, 20]. In our study, MS patients exhibited diffuse cortical q-T_2*, microstructural abnormalities indicative of myelin and/or iron loss. In both patient groups, ^{11}C-PBR28 SUVR uptake in these areas and in focal cortical lesions was significantly increased than healthy control cortical ^{11}C-PBR28 uptake. In RRMS, however,

TSPO expression in normal appearing cortex was not different from controls. These findings are in line with recent neuropathological examinations of early MS cases that have reported an elevated density of activated (CD68+) microglia in demyelinated cortical GM compared to normal cortex in patients and healthy control GM[27]. In SPMS, however, normal appearing cortex showed significant neuroinflammation, similarly to what observed in WM[7, 28, 29], suggesting that its evaluation could be used to monitor disease progression.

We used a surface-based analysis to investigate the spatial link between microglia activation and microstructural integrity along the cortex. Compared to volumetric approaches, this method improves reliability and detectability of PET cortical signal changes[30]. In RRMS, we found a widespread positive relation between q-T_2* and ^{11}C-PBR28 SUVR, indicating that the higher the microglia activation, the higher the degree of myelin and/or iron loss. Fewer regions of negative correlation were also observed in the frontal lobe. In SPMS, however, the total surface area of regions with positive correlation, which was mainly located in the temporal and parietal lobes, was smaller than the area showing a negative correlation. Interestingly, in both MS subgroups q-T_2* was pathologically increased in both areas with positive or negative correlation. These findings are open to different interpretations. The areas of negative correlation could represent chronic inactive regions of cortical demyelination with reduced number of activated microglia. It is also possible that, at some point of cortical lesion development, activated microglia might promote some degree of tissue regeneration[31]. Concurrent neuropathological/7T MRI correlations have observed that some cortical T_2* hyperintensities could represent areas of incomplete demyelination or partial remyelination[13]. Experimental and post-mortem studies demonstrate that the cortex shows a high endogenous propensity for remyelination in MS, which seems to occur regardless of disease duration or chronological patient age[32]. Finally, while increased q-T_2* reflects myelin and iron loss, local iron content increases within activated microglia could determine a decrease in q-T_2*[12]. Therefore, the negative correlation between q-T_2* and SUVR could reflect, at least in part, local prevailing effects of iron accumulation over iron loss on T_2* contrast due to extensive neuroinflammation. Future investigations could clarify this aspect[33].

There are some limitations to our study. Although surface-based analysis minimizes the spill-over from the WM and CSF, due to the different resolution of MR-PET and 7T, we cannot exclude partial volume effects. TSPO upregulation is also found during astrocyte activation[34], though neuropathological MS studies have reported that activated microglia constitute the predominant glial cell type in intracortical demyelinating lesions, which are otherwise characterized by astrocyte loss[1, 26]. Additionally, microglia activation represents only one of the multi-faceted aspects of neuroinflammation in MS[35] and, as some neuropathological observations reported minimal microglia activity in some MS cases[1, 2], future investigations will need to replicate our findings in larger cohorts. The relation between cortical and underlying WM inflammation will also need to be studied.

Acknowledgments

We would like to thank Grae Arabasz, Shirley Hsu for their technical and medical assistance with the MR-PET imaging.

Funding statement

This study was supported partly by the Clafin Award, the National MS Society (NMSS) RG-4729A2/1; RG-1802-30468), the Department of Defense (DoD) US Army W81XWH-13-1-0112 Award, and the National Institute of Health (NIH R01NS078832201 A1). Elena Herranz was supported by NMSS fellowship FG-1507-05459. Céline Louapre was supported by a fellowship from ARSEP foundation. Marco Loggia was supported by NIH 1R21NS087472-01A1, DoD W81XWH-14-1-0543, R01-NS094306-01A1, R01-NS095937-01A1, 1R01DA047088-01.

References

1. Peterson JW, Bo L, Mork S, Chang A and Trapp BD. Transected neurites, apoptotic neurons, and reduced inflammation in cortical multiple sclerosis lesions. Ann Neurol. 2001; 50: 389–400. [PubMed: 11558796]
2. Geurts JJ, Calabrese M, Fisher E and Rudick RA. Measurement and clinical effect of grey matter pathology in multiple sclerosis. Lancet Neurol. 2012; 11: 1082–92. [PubMed: 23153407]
3. Magliozzi R, Howell OW, Reeves C, et al. A Gradient of neuronal loss and meningeal inflammation in multiple sclerosis. Ann Neurol. 2010; 68: 477–93. [PubMed: 20976767]
4. Magliozzi R, Howell OW, Nicholas R, et al. Inflammatory intrathecal profiles and cortical damage in multiple sclerosis. Ann Neurol. 2018; 83: 739–55. [PubMed: 29518260]
5. Banati RB, Newcombe J, Gunn RN, et al. The peripheral benzodiazepine binding site in the brain in multiple sclerosis: quantitative in vivo imaging of microglia as a measure of disease activity. Brain. 2000; 123 (Pt 11): 2321–37. [PubMed: 11050032]
6. Politis M, Giannetti P, Su P, et al. Increased PK11195 PET binding in the cortex of patients with MS correlates with disability. Neurology. 2012; 79: 523–30. [PubMed: 22764258]
7. Herranz E, Gianni C, Louapre C, et al. Neuroinflammatory component of gray matter pathology in multiple sclerosis. Annals of neurology. 2016; 80: 776–90. [PubMed: 27686563]
8. Frischer JM, Weigand SD, Guo Y, et al. Clinical and pathological insights into the dynamic nature of the white matter multiple sclerosis plaque. Ann Neurol. 2015; 78: 710–21. [PubMed: 26239536]
9. Sethi V, Nair G, Absinta M, et al. Slowly eroding lesions in multiple sclerosis. Mult Scler. 2017; 23:464–72. [PubMed: 27339071]
10. Dal-Bianco A, Grabner G, Kronnerwetter C, et al. Slow expansion of multiple sclerosis iron rim lesions: pathology and 7 T magnetic resonance imaging. Acta Neuropathol. 2017; 133: 25–42. [PubMed: 27796537]
11. Lassmann H The pathologic substrate of magnetic resonance alterations in multiple sclerosis. Neuroimaging Clin N Am. 2008; 18: 563–76, ix. [PubMed: 19068402]
12. Kilsdonk ID, Jonkman LE, Klaver R, et al. Increased cortical grey matter lesion detection in multiple sclerosis with 7 T MRI: a post-mortem verification study. Brain : a journal of neurology. 2016; 139:1472–81. [PubMed: 26956422]
13. Louapre C, Govindarajan ST, Gianni C, et al. Beyond focal cortical lesions in MS: An in vivo quantitative and spatial imaging study at 7T. Neurology. 2015; 85: 1702–9. [PubMed: 26468411]
14. Owen DR, Yeo AJ, Gunn RN, et al. An 18-kDa translocator protein (TSPO) polymorphism explains differences in binding affinity of the PET radioligand PBR28. Journal of cerebral blood flow and metabolism : official journal of the International Society of Cerebral Blood Flow and Metabolism. 2012; 32: 1–5.
15. Parmenter BA, Testa SM, Schretlen DJ, Weinstock-Guttman B and Benedict RH. The utility of regression-based norms in interpreting the minimal assessment of cognitive function in multiple sclerosis (MACFIMS). J Int Neuropsychol Soc. 2010; 16: 6–16. [PubMed: 19796441]
16. Kolb A, Wehrl HF, Hofmann M, et al. Technical performance evaluation of a human brain PET/MRI system. European radiology. 2012; 22: 1776–88. [PubMed: 22752524]
17. van der Kouwe AJW, Benner T, Salat DH and Fischl B. Brain morphometry with multiecho MPRAGE. Neuroimage. 2008; 40: 559–69. [PubMed: 18242102]
18. Izquierdo-Garcia D, Hansen AE, Forster S, et al. An SPM8-based approach for attenuation correction combining segmentation and nonrigid template formation: application to simultaneous

PET/MR brain imaging. Journal of nuclear medicine : official publication, Society of Nuclear Medicine. 2014; 55: 1825–30.

19. Cohen-Adad J, Polimeni JR, Helmer KG, et al. T* mapping and B orientation-dependence at 7 T reveal cyto- and myeloarchitecture organization of the human cortex. Neuroimage. 2012; 60: 1006–14. [PubMed: 22270354]
20. Mainero C, Louapre C, Govindarajan ST, et al. A gradient in cortical pathology in multiple sclerosis by in vivo quantitative 7 T imaging. Brain : a journal of neurology. 2015; 138: 932–45. [PubMed: 25681411]
21. Herranz E, Hooker JM, Izquierdo-Garcia D, Loggia ML and Mainero C. Reply. Annals of neurology. 2016.
22. Stankoff B, Poirion E, Tonietto M and Bodini B. Exploring the heterogeneity of MS lesions using positron emission tomography: a reappraisal of their contribution to disability. Brain Pathol. 2018; 28: 723–34. [PubMed: 30020560]
23. Kreisl WC, Lyoo CH, Liow JS, et al. (11)C-PBR28 binding to translocator protein increases with progression of Alzheimer's disease. Neurobiol Aging. 2016; 44: 53–61. [PubMed: 27318133]
24. Alshikho MJ, Zurcher NR, Loggia ML, et al. Integrated magnetic resonance imaging and [(11) C]-PBR28 positron emission tomographic imaging in amyotrophic lateral sclerosis. Ann Neurol. 2018; 83: 1186–97. [PubMed: 29740862]
25. Zrzavy T, Hametner S, Wimmer I, Butovsky O, Weiner HL and Lassmann H. Loss of 'homeostatic' microglia and patterns of their activation in active multiple sclerosis. Brain. 2017; 140: 1900–13. [PubMed: 28541408]
26. Lucchinetti CF, Popescu BF, Bunyan RF, et al. Inflammatory cortical demyelination in early multiple sclerosis. The New England journal of medicine. 2011; 365: 2188–97. [PubMed: 22150037]
27. Bevan RJ, Evans R, Griffiths L, et al. Meningeal inflammation and cortical demyelination in acute multiple sclerosis. Ann Neurol. 2018; 84: 829–42. [PubMed: 30362156]
28. Kutzelnigg A, Lucchinetti CF, Stadelmann C, et al. Cortical demyelination and diffuse white matter injury in multiple sclerosis. Brain. 2005; 128: 2705–12. [PubMed: 16230320]
29. Rissanen E, Tuisku J, Rokka J, et al. In Vivo Detection of Diffuse Inflammation in Secondary Progressive Multiple Sclerosis Using PET Imaging and the Radioligand (1)(1)C-PK11195. Journal of nuclear medicine : official publication, Society of Nuclear Medicine. 2014; 55: 939–44.
30. Greve DN, Svarer C, Fisher PM, et al. Cortical surface-based analysis reduces bias and variance in kinetic modeling of brain PET data. NeuroImage. 2014; 92: 225–36. [PubMed: 24361666]
31. Hamelin L, Lagarde J, Dorothee G, et al. Distinct dynamic profiles of microglial activation are associated with progression of Alzheimer's disease. Brain. 2018; 141: 1855–70. [PubMed: 29608645]
32. Staugaitis SM, Chang A and Trapp BD. Cortical pathology in multiple sclerosis: experimental approaches to studies on the mechanisms of demyelination and remyelination. Acta Neurol Scand Suppl. 2012: 97–102. [PubMed: 23278664]
33. Mangeat G, Govindarajan ST, Mainero C and Cohen-Adad J. Multivariate combination of magnetization transfer, T2* and B0 orientation to study the myelo-architecture of the in vivo human cortex. NeuroImage. 2015; 119: 89–102. [PubMed: 26095090]
34. Lavisse S, Guillermier M, Herard AS, et al. Reactive astrocytes overexpress TSPO and are detected by TSPO positron emission tomography imaging. J Neurosci. 2012; 32: 10809–18. [PubMed: 22875916]
35. Mallucci G, Peruzzotti-Jametti L, Bernstock JD and Pluchino S. The role of immune cells, glia and neurons in white and gray matter pathology in multiple sclerosis. Prog Neurobiol. 2015; 127-128: 1–22. [PubMed: 25802011]

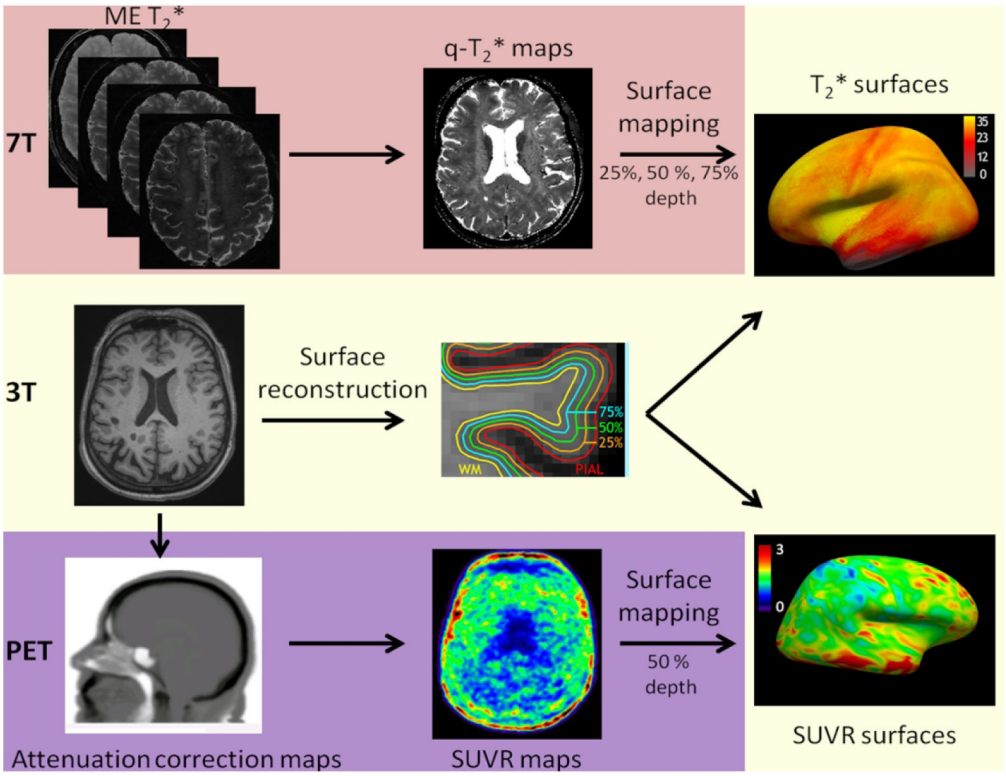

Figure 1.

Imaging analysis pipeline. Seven Tesla (7T) quantitative multi-echo (ME) T_2* cortical maps were obtained voxel-wise using Levenberg–Marquardt non-linear regression. Anatomical 3T magnetization-prepared rapid acquisition with multiple gradient echoes (MEMPR) images was processed using FreeSurfer to reconstruct cortical surfaces.

Quantitative T_2* maps were registered to the cortical surfaces, sampled at 25%, 50%, and 75% depths from the pial surface and normalized into a common ‘fsaverage’ space. Normalized 60-90 minutes standardized uptake value (SUVR) maps (1.25 mm isotropic voxels) were registered to cortical surfaces and sampled at 50% depth from the pial surface.

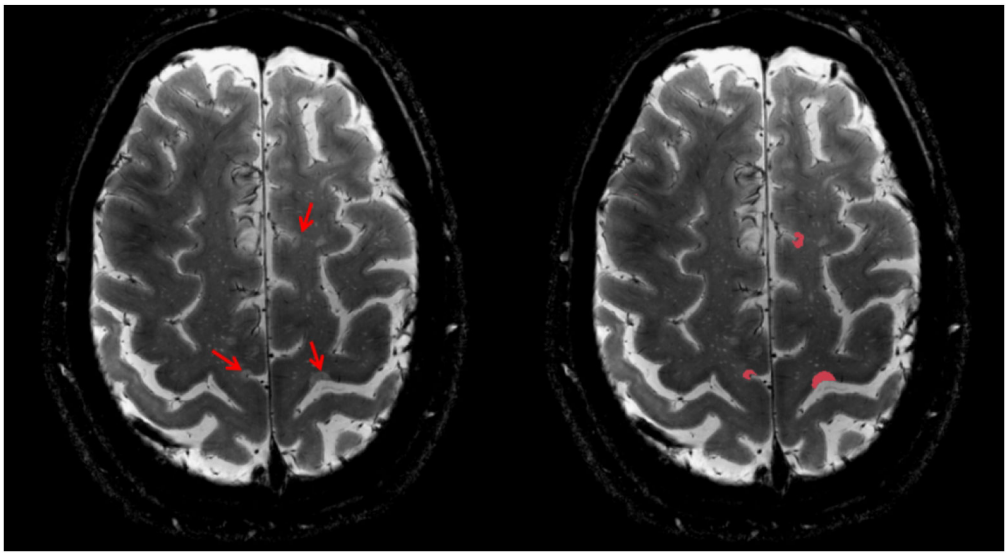

Figure 2.
Axial 7 Tesla T_2* weighted image shows examples of cortical lesions (red arrows) in a 59-year old SPMS patient (left) and the segmentation of the lesions with Slicer v4.2.0 (right).

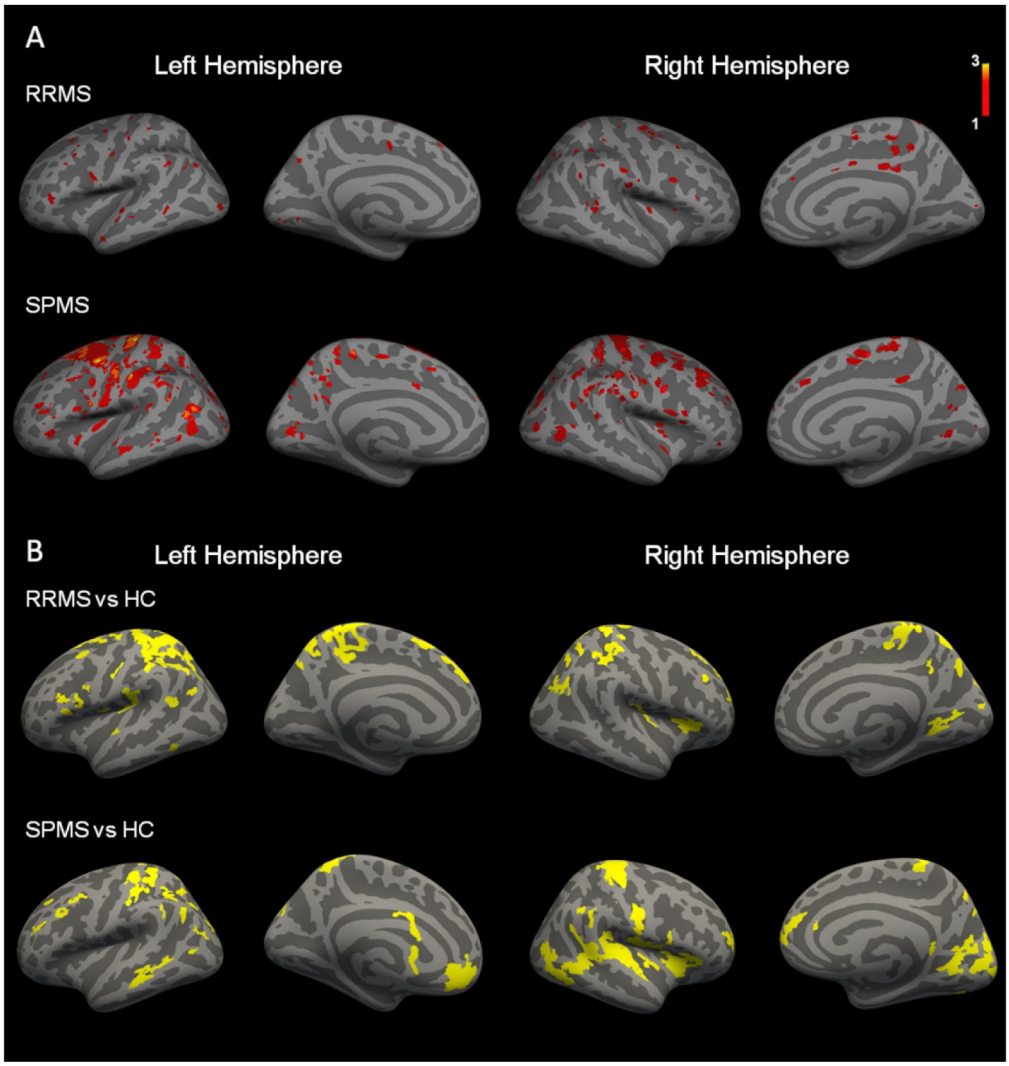

Figure 3.

(A) Cortical lesions distribution maps. Overlay on 'fsaverage' template of cortical lesion distribution maps in relapsing remitting and secondary progressive multiple sclerosis (RRMS, SPMS) patients. The color overlay represents the number of cortical lesion occurrence. (B) Differences in quantitative T_2* at 7 Tesla between relapsing remitting and secondary progressive multiple sclerosis (RRMS, SPMS) patients and healthy controls (HC). Overlay of the general linear model (GLM) significance maps ($p<0.05$ corrected for multiple comparisons) showing the combined cortical regions of increased quantitative T_2* at 25%, 50%, and 75% depth from the pial surface in patients relative to healthy controls.

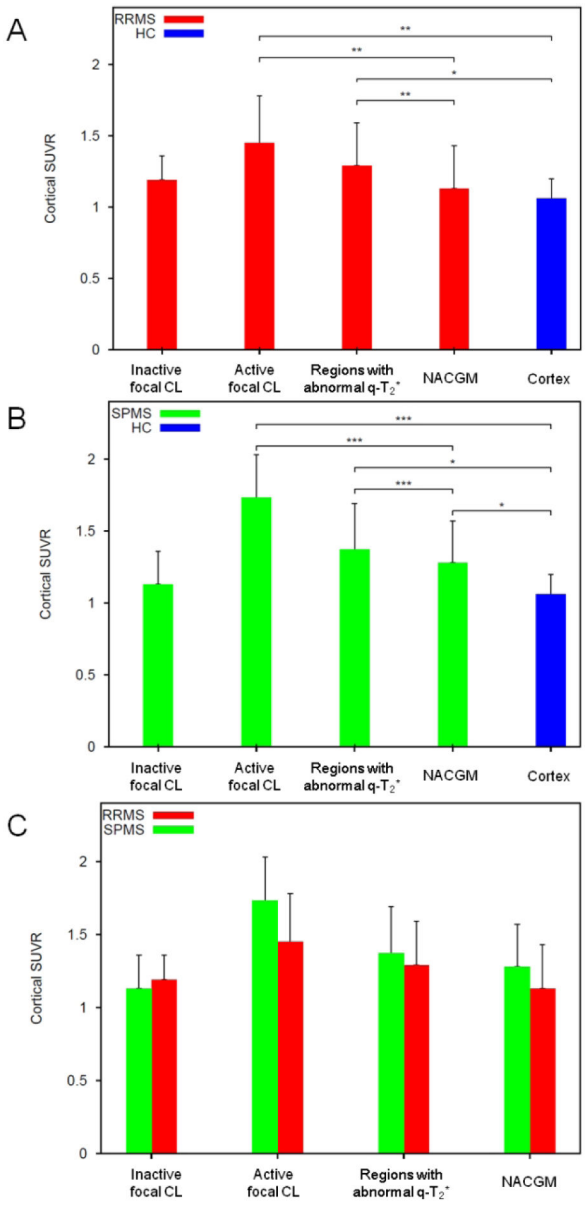

Figure 4.

Histograms showing mean normalized ^{11}C-PBR28 standardized uptake values (SUVR) in cortical tissue compartments in relapsing remitting and secondary progressive multiple sclerosis (RRMS, SPMS) patients, and healthy controls (HC). In RRMS and SPMS, mean ^{11}C-PBR28 SUVR within active cortical lesions, and cortical regions showing significant quantitative T_2* differences in patients versus HC were higher than mean “C-PBR28 SUVR in normal appearing cortex, by paired t-test. No significant differences were found between inactive cortical lesions and normal appearing cortex. SPMS showed higher mean ^{11}C-PBR28 SUVR in normal appearing cortex relative to mean cortical SUVR in HC, by multivariate linear regression including age and affinity as nuisance factors. No significant differences were found between subgroups in mean ^{11}C-PBR28 SUVR in active or inactive cortical lesions, and in regions showing significant quantitative T_2* differences in patients

versus HC or normal appearing cortex, by multivariate linear regression including age and affinity as nuisance factors.

*: $p<0.05$; **: $p<0.005$; ***$p<0.0005$.

NACGM: normal appearing cortical grey matter; RRMS: relapsing remitting multiple sclerosis; SPMS: secondary progressive multiple sclerosis; HC: Healthy Controls.

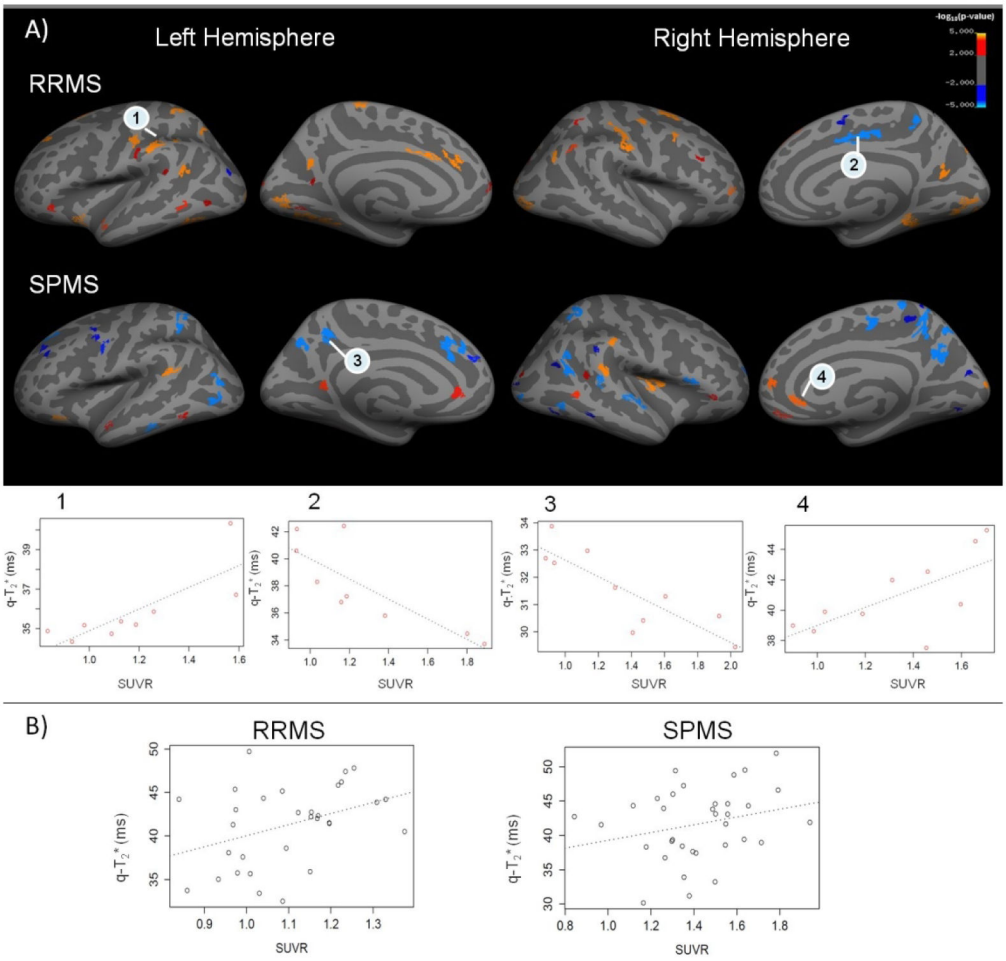

Figure 5.

A) Areas of correlation between cortical quantitative T_2* (q-T_2*) at 7 Tesla (7T) and ^{11}C-PBR28 standarized uptake values (SUVR) in relapsing remitting and secondary progressive multiple sclerosis (RRMS, SPMS) patients. Overlay of the general linear model (GLM) significance maps ($p<0.05$ corrected for multiple comparisons) showing cortical areas with a positive (red orange yellow) or negative (blue) correlation between q-T_2* and ^{11}C-PBR28 SUVR at 50% depth from the pial surface in RRMS and SPMS subjects (Top). Adjustment variables included in the model were age and affinity binding. Examples of plots of correlation between q-T_2* and ^{11}C-PBR28 SUVR in some regions exhibiting a statistical significance at the GLM analysis ($p<0.05$) (Bottom). B) Examples of plots showing, at the individual patient level in a 48 years-old RRMS (left) and a 40 years-old SPMS (right) subject, the association between ^{11}C-PBR28 SUVR and q-T_2* in focal cortical lesions identified at 7T. Both metrics (^{11}C-PBR28 SUVR and q-T_2*) were sampled at 50% depth from the pial surface.

Tablel 1.

Demographic, clinical, and MRI data in the whole multiple sclerosis cohort, and in patients grouped according to their disease phenotype, and their profile of cortical lesion inflammatory activity.

	HC (n= 31)	All MS (n= 19)	RRMS (n= 9)	SPMS (n= 10)	High CL Activity (n= 10)	Low CL Activity (n= 9)
Demographics and clinic						
Gender (F/M)	16/15	(15/3)	(8/1)	(7/3)	(8/2)	(7/2)
Age, years mean (SD)	42 (10)	48 (10)	43 (10)	52 (8)	52 (9)	43 (9)
HAB/MAB	7/7	(11/8)	(5/4)	(6/4)	(5/5)	(5/4)
RRMS/SPMS	-	NA	NA	NA	3/7	6/3
EDSS, median [range]	-	4 [2- 7.5]	2 [2 - 6]	6.5 [2.5 - 7.5]	6.5 [2 – 7.5]	2.5 [2.5 - 6.5]
SDMT Z score, mean (SD)	-	−0.18 (1.98)	1.20 (1.15)	−1.23 (1.8)	−1.0 (2.2)	0.9 (0.9)
Disease duration, years, median [range]	-	13.5 [1-40]	2 [1-33]	26 [7-40]	18.5 [2-36]	5 [1-40]
DMT	-	14/19	7/9	7/10	6/10	8/9
MRI metrics						
Total cortical lesion volume, mm^3 mean (SD)	-	2304 (3571)	685 (718)	3600 (4415)	3646 (4386)	558 (671)
Intracortical lesion volume, mm^3 mean (SD)	-	748 (1041)	463 (605)	976 (1278)	1070 (1231)	307 (567)
Leukocortical lesion volume, mm^3 mean (SD)	-	1557 (2712)	222 (199)	2624 (3319)	2575 (3356)	251 (232)
Total cortical lesion count, median [range]	-	10.5 [1-164]	8 [2-39]	19 [1-164]	24 [7-164]	6 [1-39]
Intracortical lesion count, median [range]	-	7.5 [0-40]	5 [0-32]	14.5 [0-40]	15 [3-40]	0 [0-32]
Leukocortical lesion count, median [range]	-	3.5 [1-144]	3 [1-7]	5 [1-144]	4 [1-144]	3 [1-7]
White matter lesion volume, mm^3mean (SD)	-	7720 (8324)	3750 (3731)	10895 (9738)	8383 (8578)	6185 (8229)
Cortical thickness, mm^2, mean (SD)	2.56 (0.17)	2.34 (0.08)	2.35 (0.06)	2.32 (1.10)	2.33 (0.09)	2.34 (0.07)

RRMS= relapsing-remitting MS; SPMS= secondary-progressive MS; SD= standard deviation; HAB= high affinity binders; MAB= mixed affinity binders; n= number; DTM= Disease Modifying Treatment, EDSS= Expanded Disability Status Scale; SDMT=Symbol Digit Modalities Test; CL= Cortical Lesion; SD= standard deviation; HAB= high affinity binders; MAB= mixed affinity binders; n= number.

Table 2.

Mean normalized ^{11}C-PBR28 uptake in cortical tissue compartments in relapsing remitting and secondary progressive multiple sclerosis (RRMS, SPMS) patients and healthy controls.

Region	**Mean ± SD ^{11}C-PBR28 SUVR**		
	RRMS	SPMS	HC
Active focal CL	1.4 ± 0.3	1.7 ± 0.3	-
Regions with abnormal q-T_2*	1.3 ± 0.3	1.4 ± 0.3	-
NACGM	1.1 ± 0.3	1.3 ± 0.3	-
Cortex	-	-	1.1 ± 0.1
	P-value		**Test**
	RRMS	SPMS	
Active focal CL vs NACGM	0.002	$9{\cdot}10^{-5}$	Paired t-test
Regions with abnormal q-T_2* vs NACGM	0.001	0.004	Paired t-test
Active focal CL vs HC Cortex	0.0017	$2{\cdot}10^{-5}$	Multivariate linear regression
Regions with abnormal q-T_2* vs HC Cortex	0.05	0.01	Multivariate linear regression
NACGM vs HC cortex	0.09	0.05	Multivariate linear regression

CL= Cortical lesions; HC= healthy controls; NACGM= Normal appearing cortical grey matter; SD= standard deviation; SUVR= normalized standardized uptake values.

Age and binding affinity were included as adjustment variables in all multivariate linear regression analyses.

Table 3.

Location, surface area (S) and percentage of the total cortical surface area (%) of regions exhibiting a significant positive or negative correlation (P< 0.05, corrected) between 7 Tesla quantitative T_2* and ^{11}C-PBR28 uptake at mid-cortical depth in relapsing remitting and secondary progressive multiple sclerosis (RRMS, SPMS) patients.

Left hemisphere	Right hemisphere
RRMS	
Positive correlation	
Superior frontal – pars orbitalis	Superior frontal – rostral and caudal middle frontal
Superior, middle and inferior temporal - insula	Inferior temporal – insula
Inferior and superior parietal - caudal anterior and posterior cingulate – supramarginal – precuneus	Precuneus - inferior and superior parietal - supramarginal
Lateral occipital – lingual – fusiform	Lingual - lateral occipital – fusiform
Precentral - postcentral	Precentral - postcentral
S = 2709 mm^2 (4.1 %)	**S = 2453 mm^2 (3.8%)**
Negative correlation	
Rostral middle frontal	Superior - rostral middle frontal
Inferior parietal	Precuneus, superior parietal - posterior and isthmus cingulated
	Precentral
S = 95 mm^2 (0.1 %)	**S = S = 454 mm^2 (0.7 %)**
SPMS	
Positive correlation	
Superior frontal - lateral orbito frontal - parsopercularis	Superior frontal - lateral and medial orbito frontal - parstriangularis - pars orbitalis
Inferior and superior temporal	Insula – Superior and middle temporal - temporal pole
Supramarginal - isthmuscingulate - fusiform Inferior parietal – supramarginal- rostral anterior cingulate	
	Lateraloccipital - cuneus
S = 385 mm^2 (0.6 %)	**S = 1158 mm^2 (1.7 %)**
Negative correlation	
Superior frontal, rostral and caudal middle frontal	Rostral middle frontal - parsopercularis
Inferior temporal	Inferior temporal - bankssts
Inferior and superior parietal – precuneus - rostral anterior cingulate	Superior and inferior parietal - supramarginal - precuneus
Lateral occipital	Lateral occipital – fusiform – lingual - cuneus
Precentral	Precentral - paracentral
S = 1466 mm^2 (2.2 %)	**S = 2150 mm^2 (3.3 %)**

Table 4.

Comparisons of quantitative T_2* (q-T_2*) values extracted from cortical regions with a negative or a positive association with ^{11}C-PBR28 standardized uptake values (SUVR) in relapsing remitting and secondary progressive multiple sclerosis (RRMS, SPMS) patients relative to healthy controls (HC).

	q- T_2* (ms) at 7Tesla mean (SD)		
Cortical region with abnormal q-T_2*	**RRMS**	**HC**	**p-value**
Positive	35.0 (1.7)	32.6 (1.6)	0.0006 *
Negative	34.0 (2.6)	32.1 (1.8)	0.001 *
	SPMS	**HC**	
Positive	33.1 (0.9)	30.8 (1.8)	0.0007 *
Negative	34.3 (1.9)	32.2 (1.7)	0.004 *

* By multilinear regression, adjusting for age.